JOURNAL OF MATERIALS SCIENCE 21 (1986) 1166–1170

Stress corrosion cracking behaviour of the duplex Fe–10 Al–29 Mn–0.4 C alloy in 20% NaCl solution at 100° C

S. C. TJONG
Institute of Materials Science and Engineering, National Sun Yat-Sen University, Kaohsiung, Taiwan

The stress corrosion cracking behaviour of the duplex Fe–10 Al–29 Mn–0.4 C alloy having two phases (α and γ) in an aqueous 20% NaCl solution (100° C) has been investigated using both the static constant load and dynamic slow strain rate tests. The constant load test shows that the duplex alloy investigated is immune to stress corrosion cracking in a 20% NaCl solution. However, the slow strain-rate test reveals that this alloy is susceptible to stress corrosion cracking at the stabilized corrosion potential, and also at potentials anodic and cathodic to this potential. Furthermore, the metallographic cross section of this duplex alloy after slow strain-rate testing shows that the secondary cracks propagate transgranularly through the ferrite grains at and above the stabilized corrosion potential. However, the cracks propagate transgranularly in both the ferrite and austenite grains and also at the austenite–ferrite grain boundaries when the applied potential is cathodic to the stabilized corrosion potential.

1. Introduction

The Fe–Al–Mn alloy system is a type of austenitic stainless steel with aluminium and manganese replacing chromium and nickel, respectively, in the conventional Fe–Cr–Ni stainless steel. Chromium and nickel are strategic materials which are expensive in some countries, particularly chromium, since about 95% of the world reserves are located in South Africa and Zimbabwe. However, aluminium is plentiful and available at a relatively cheap cost and therefore shows promise to replace chromium in the conventional stainless steel. Aluminium is well known as a ferrite stabilizer and the addition of this element to the alloy system can increase the alloy's corrosion and oxidation resistance. However, manganese is added to stabilize the austenite structure which shows good hot workability and ductility. Carbon is generally also added to increase austenite stability and the addition of up to 1% carbon contributes to the strength of the alloy significantly [1]. The Fe–Al–Mn alloy system can be further strengthened by ageing heat-treatment and this alloy system was reported to be approximately 20% lighter than the conventional stainless steel [2]. The Fe–Al–Mn alloy was also considered as a potential new cryogenic alloy due to its excellent mechanical properties at low temperatures [3]. The Fe–Al–Mn alloy system has been shown to exhibit good oxidation resistance at temperatures up to 850° C [4].

As has been well documented, the concentrations of manganese and aluminium are sensitive to the corrosion resistance and mechanical properties of the Fe–Al–Mn alloy [5]. From the Fe–Al–Mn phase diagrams [6, 7], high concentration of manganese (> 35%) tends to embrittle the alloy due to the formation of the β-manganese phase. On the other hand, concentrations of aluminium greater than about 12% could lead to the formation of the ferritic stainless alloy. According to the work of Kayak [8], the optimal composition of the Fe–Al–Mn alloy system showing good physicomechanical properties should contain about 8 to 10% Al and 25 to 30% Mn.

In recent years, duplex stainless steels and, in particular, the austenitic–ferritic grades are beginning to attract considerable attention for use in seawater environments due to their excellent localized corrosion resistance. In addition, the duplex steels also possess high strength and toughness, and hence good fabrication properties. In the carbon containing Fe–10 Al–29 Mn alloy system, the duplex microstructure can be developed by lowering the carbon content of the alloy to less than about 0.5%.

It is generally agreed that stress corrosion cracking (SCC) is one of the most frequent causes of failure of the austenitic stainless steels in chloride-containing environments. The environment-assisted cracking often limits the use of the austenitic stainless steels in these chloride-containing environments. However, the duplex (austenitic-ferritic) steels are superior to conventional austenitic stainless steels in resistance to SCC [9]. Most of the laboratory tests on SCC have been performed by either static constant load or dynamic slow strain-rate methods. There appears to be no previous work reported in the literature on the SCC behaviour of duplex Fe–Al–Mn stainless steel. The present work investigates the SCC behaviour of the duplex Fe–10 Al–29 Mn–0.4 C alloy in 20% NaCl solution by using constant load and slow strain-rate techniques.

0022–2461/86 $03.00 + .12

TABLE I Chemical composition of the tested duplex alloy (wt %)

Alloy	C	Al	Mn	Si	P	S	Fe
Fe–10 Al–29 Mn–0.4 C	0.39	10.6	29.6	0.11	0.01	0.024	Bal.

2. Experimental procedure

The alloy investigated was prepared by melting high purity iron, aluminium and manganese in a laboratory induction furnace, and was then cast into a steel mould. The cast ingot was hot forged at 1200° C into a billet. This billet was homogenized at 1100° C for 12 h, air cooled and subsequently cold rolled to 2 mm thick plates. Tensile specimens were machined from the resultant plates according to the DIN 50125 specification (Fig. 1). These tensile specimens were then solution treated at 1050° C for 2 h and immediately quenched into water upon removal from the furnace. Details of the chemical composition and mechanical properties of the solution treated specimen are given in Tables I and II.

The electrochemical glass cell used permitted the introduction of a tensile specimen, a platinum counter electrode, a condenser, a thermometer and a capillary which was connected to a beaker in which a silver–silver chloride (4 K mol m^{-3}) reference electrode was placed. This cell was used for both constant load and slow strain rate tests. The test solution was made from reagent grade NaCl and distilled water. An ECO potentiostat model 553 was used to control the potential of the specimen.

The gauge length of the specimen was abraded down to 600 grit, it was then degreased with acetone, and washed with distilled water. The non-gauge part of the tensile specimen was covered with teflon tape and finally the teflon–specimen interface was covered with silicone glue.

The susceptibility of the Fe–10 Al–29 Mn–0.4 C alloy to SCC in a 20% NaCl solution at 100° C was studied at different constant potentials using the constant load and slow strain-rate methods. In both tests, as the solution temperature reached 100° C, the open circuit corrosion potential was recorded with an X–Y recorder until a stabilized potential was reached. In the constant load test, all SCC specimens were stressed to 90% of the yield strength. The loads and potential control were applied after a stable corrosion potential has been achieved.

The slow strain-rate method was conducted with an Instron universal testing machine model 1125. The cross-head speed used was 10^{-4} mm sec^{-1}, corresponding to a nominal tensile strain of 2.5×10^{-6} sec^{-1}. After testing, the fracture surface of the specimen was ultrasonically cleaned in acetone in order to remove the corrosion products, and was subsequently examined in the scanning electron microscope. The longitudinal section of the specimen near the fracture surface was also examined metallographically using the optical microscope.

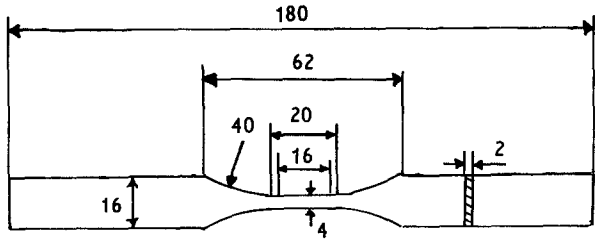

Figure 1 Tensile test specimen according to DIN specification 50125 (dimensions in mm).

3. Results and discussion

Fig. 2 shows the microstructure of the solution-treated Fe–10 Al–29 Mn–0.4 C duplex alloy. The dark areas in the micrograph are the austenite phase (γ) whereas the light areas are the ferrite phase (α). The alloy shown in Fig. 2 contains about 40 to 50% of α in a γ matrix. Fig. 3 shows the polarization curves of the duplex alloy generated after 1 and 17 h immersion in a 20% NaCl solution at 100° C. In a microstructure containing two phases, the polarization curve indicates the pitting potential of each of these phases (curve I).

Fig. 4 shows the influence of time on the open circuit corrosion potential of the duplex alloy in a 20% NaCl solution at 100° C. The open circuit corrosion potential is the corrosion potential of a specimen measured against a reference electrode in such a way that there is no external source of current. This potential reaches a stabilized value (E_{oc}) after immersion in a solution for several hours. The corrosion potential was initially located at -600 mV and reached the stabilized potential at -514 mV after the specimen had been immersed about 17 h in the NaCl solution. Staehle *et al.* [10] reported that a protective passive film was formed on the specimen surface at the stabilized corrosion potential. It has long been known that a critical potential exists for the stainless steels in chloride solutions which separates the range of potentials suceptible to SCC from those immune to SCC [11]. The stainless steel is suceptible to SCC when its corrosion potential is noble to its critical potential (E_{cc}) and immune when cathodic [12]. Fig. 5 shows the effect of applied potential on time to failure (TTF) of the duplex alloy in 20% NaCl solution. As can be seen in this figure, the stabilized corrosion potential is cathodic to the E_{cc}. As a result, the duplex alloy is immune to SCC in NaCl solution.

In the present work, the duplex alloy investigated was found to be resistant to SCC under static test conditions. However, the constant load test only considered the combined effect of a static tensile stress and a corrosive environment in the absence of severe plastic deformation. In addition, the constant load

TABLE II Mechanical properties of the duplex alloy investigated

Alloy	0.2% proof stress (kg mm^{-2})	Tensile strength (kg mm^{-2})	Elongation (%)
Fe–10 Al–29 Mn–0.4 C	48.89	85.26	45.3

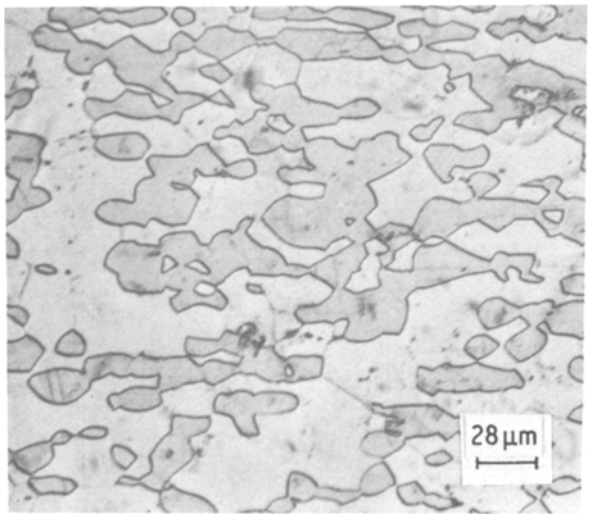

Figure 2 Photomicrograph of the solution-treated duplex Fe–10 Al–29 Mn–0.4 C alloy. The etch used was 10% nital.

test shows poor data reproducibility and required a longer incubation time for the initiation of a crack. Therefore, the dynamic slow strain technique has been increasingly used recently to determine the susceptibility of an alloy to SCC. The advantage of the slow strain test is that it can maintain repetitive rupture of the passive films by virtue of its continuous application of strain. Acceleration dissolution then takes place at the slip-steps due to the moving dislocations emerging at the specimen surface during continuous straining.

Fig. 6 shows a scanning electron micrograph of the fracture surface of the duplex alloy investigated in air after slow strain-rate testing. It can be seen that the fracture surface exhibits the dimpled structure which is associated with the nucleation, growth and coalescence of the microvoids. Fig. 7 shows the scanning electron fractograph of the duplex alloy fractured in a 20% NaCl solution at the stabilized corrosion potential. The fracture surface produced by the slow strain rate test at the stabilized corrosion potential exhibits flat cleavage facets along with the presence of the secondary cracks. This cleavage morphology is

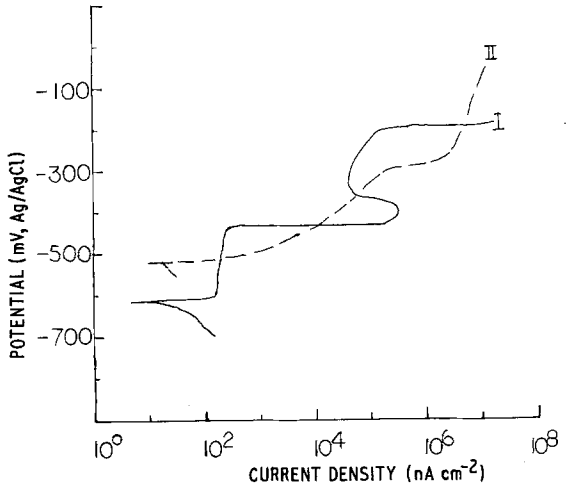

Figure 3 Polarization curves of the duplex alloy generated after 1 h (curve I) and 17 h (curve II) immersion in a 20% NaCl solution at 100° C. Scanning rate 1 mV sec^{-1}.

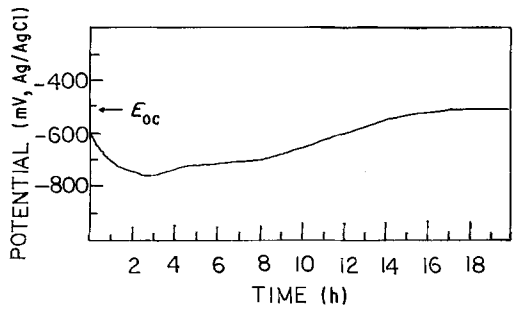

Figure 4 Open circuit corrosion potential against time for the Fe–10 Al–29 Mn–0.4 C alloy immersed in a 20% NaCl solution at 100° C.

characteristic of transgranular SCC failure. The ultimate tensile strength and elongation of the duplex alloy were found to be much less in a 20% NaCl solution at the stabilized corrosion potential than when tested in air. The tensile strength and elongation of the duplex alloy were found to be 50.2 kg mm^{-2} and 2%, respectively, when tested in a 20% NaCl solution at 100° C.

As the potential was applied anodically to the stabilized corrosion potential, the scanning electron micrograph showed a similar transgranular pattern of cleavage facets as in Fig. 7. This indicates that SCC occurs in duplex stainless steel at potentials at and above the stabilized corrosion potential under slow strain-rate testing conditions.

Fig. 8 shows the metallographic micrograph of the longitudinal cross section of the duplex alloy which failed at the applied potential of −490 mV. It is obvious from this micrograph that the secondary cracks propagate transgranularly through the ferrite grains. It has been reported that the SCC resistance of the duplex stainless steel increases as the volume per cent of ferrite increases [13]. It is believed that the improved SCC resistance of the duplex stainless steel is associated with the mechanical keying effect of the ferrite phase [13], and the electrochemical galvanic effect between the ferrite and austenite [14]. Hochmann *et al.* [14] reported that ferrite was more anodic than the austenite in the duplex stainless steel. At low stresses, only the austenite is strained. The ferrite, which is not deformed, cathodically protects the austenite phase. However, the ferrite phase undergoes mechanical depassivation at high stresses due to

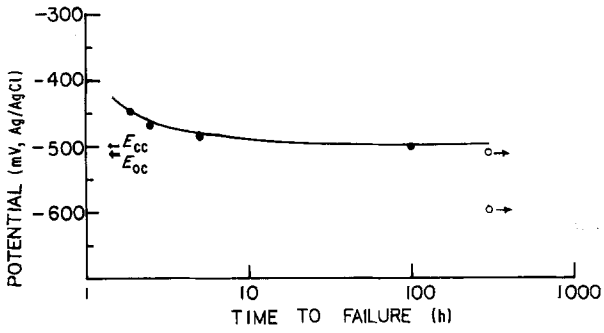

Figure 5 Effect of applied potential on the time to failure of the Fe–10 Al–29 Mn–0.4 C alloy in a 20% NaCl solution. Stressed to 90% of the yield strength.

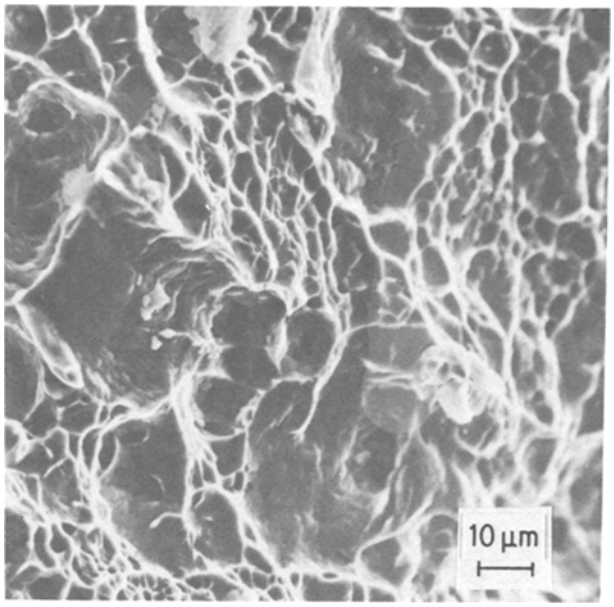

Figure 6 Fracture surface of the Fe–10 Al–29 Mn–0.4 C alloy after slow strain-rate testing in air.

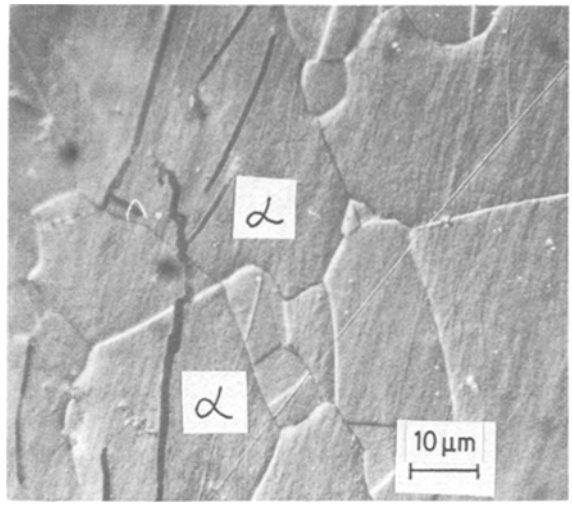

Figure 8 Photomicrograph of the longitudinal cross section of the Fe–10 Al–29 Mn–0.4 C alloy which failed in a 20% NaCl solution (100° C) at the applied potential of −490 mV.

the plastic straining. As a result, cracks propagate transgranularly through the ferrite grains.

Fig. 9 shows the scanning electron fractograph of the duplex alloy after slow strain-rate testing at −600 mV. As can be seen, the duplex alloy failed in the mixed transgranular and intergranular cracking modes. At this potential, bubbles of hydrogen can be seen evolving from the specimen surface during straining. As the potential was further applied cathodically to −700 mV, the fractograph showed a similar mixed modes cracking manner. It has been mentioned previously that failure will not occur at the applied potential of −600 mV under the static constant load test. However, the continuous production of the bare metal surfaces during the slow strain-rate test enables sufficient amounts of hydrogen to be

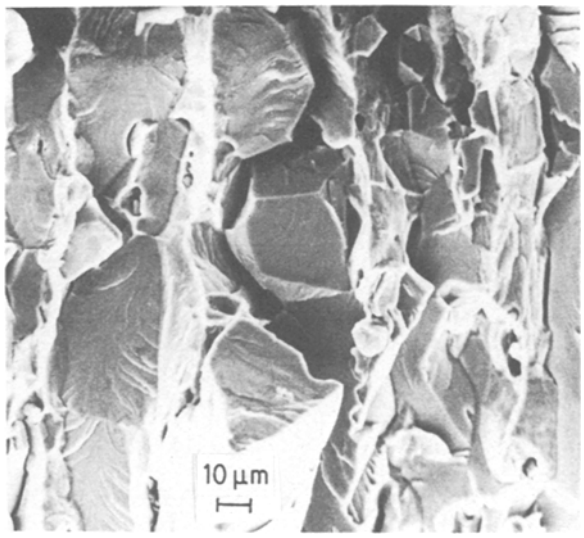

Figure 9 Scanning electron fractograph of the Fe–10 Al–29 Mn–0.4 C alloy after slow strain-rate testing in a 20% NaCl solution (100° C) at the applied potential of −600 mV.

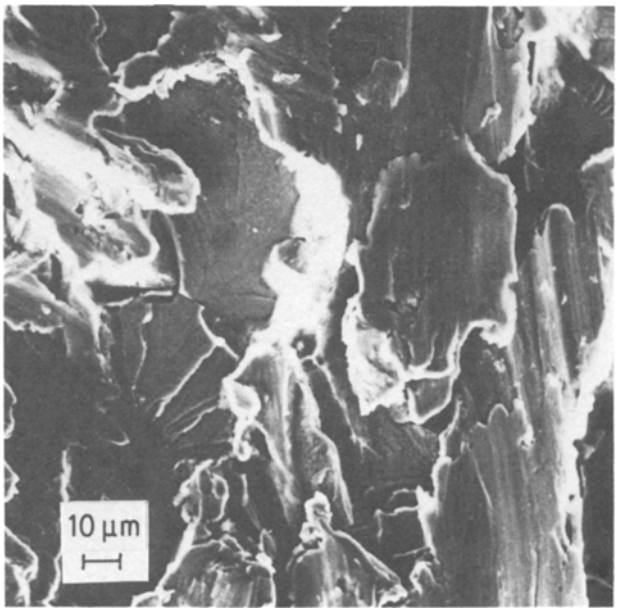

Figure 7 Scanning electron fractograph of the Fe–10 Al–29 Mn–0.4 C alloy after slow strain-rate testing in a 20% NaCl solution (100° C) at the stabilized corrosion potential.

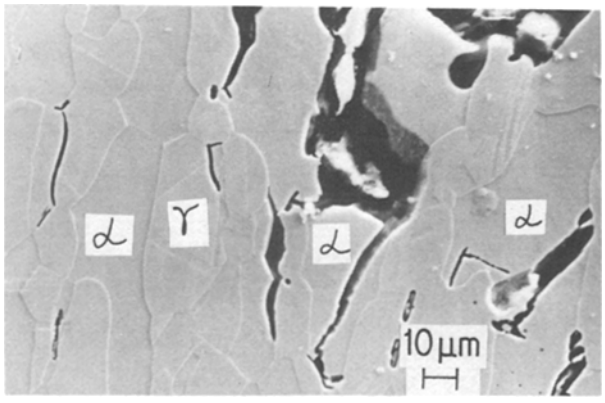

Figure 10 Photomicrograph of the longitudinal cross section of the Fe–10 Al–29 Mn–0.4 C alloy which failed in a 20% NaCl solution at the applied potential of −600 mV.

transported into the specimen. The longitudinal cross section of the specimen which failed at −600 mV is shown in Fig. 10. The hydrogen-induced cracks were observed to propagate through both the austenite and ferrite grains, and the austenite–ferrite grain boundaries.

4. Conclusion

The present work has shown that the duplex Fe–10 Al–29 Mn–0.4 C alloy is immune to SCC in a 20% NaCl solution at 100° C during the constant load test. However, the accelerated slow strain-rate test reveals that this duplex alloy is susceptible to SCC at the stabilized potential and also at potentials anodic and cathodic to this stabilized corrosion potential.

Acknowledgements

This work was supported by the National Science Council through Grant no. NSC 74-0201-E110-01. The author would like to thank Professor C. M. Wan of National Tsing Hua University for kindly providing the duplex alloy.

References

1. D. J. SCHMATZ, *Trans. ASM.* **52** (1960) 898.
2. J. L. HAM and R. E. CAIRNS Jr, *Prod. Eng.* **29** (1958) 50.
3. J. CHARLES, A. BERGHEZAN, A. LUTTS and P. L. DANCOISNE, *Metal Prog.* **116** (1981) 71.
4. J. C. GARCIS, N. ROSAS and K. RIOJA, *ibid.* **117** (1982) 47.
5. P. TOMASZEWICZ and G. R. WALLWORK, *Corrosion* **40** (1984) 152.
6. D. J. SCHMATZ, *Trans. Met. Soc. AIME* **215** (1959) 112.
7. V. G. RIVLIN, *Int. Met. Rev.* **28** (1983) 309.
8. G. L. KAYAK, *Met. Sci. Heat Treat.* **2** (1969) 95.
9. R. A. LULA (ed.), "Duplex Stainless Steel" (American Society for Metals, Ohio, 1982) p. 267.
10. R. W. STAEHLE, J. J. ROYEULA, R. L. RAREDON, E. SERRATE, C. R. MORIN and R. V. FARRAR, *Corrosion* **26** (1970) 451.
11. S. BARNATT and D. VAN ROOYEN, *J. Electrochem. Soc.* **108** (1961) 222.
12. H. H. UHLIG and E. W. COOK, *ibid.* **116** (1969) 173.
13. M. G. FONTANA, F. H. BECK, J. W. FLOWERS, *Met. Prog.* **96** (1961) 99.
14. J. HOCHMANN, A. DESESTRET, R. JOLLY and R. MAYOND, in Proceedings of the International Conference on Stress Corrosion Cracking and Hydrogen Embrittlement of Iron Base Alloys, Unieux-Firminy, France, June 1973 (National Association of Corrosion Engineers, 1977) p. 956.

Received 13 March
and accepted 30 May 1985